Princeton Plasma Physics Laboratory

Dependence of Recycling and Edge Profiles on Lithium Evaporation in High Triangularity, High Performance NSTX H-mode Discharges

R. Maingi, T.H. Osborne, M.G. Bell, R.E. Bell, D.P. Boyle, J.M. Canik,
A. Diallo, R. Kaita, S.M. Kaye, H.W. Kugel, B.P. LeBlanc,
S.A. Sabbagh, C.H. Skinner, V.A. Soukhanovskii,
and the NSTX team

May 2014

PRINCETON
PLASMA PHYSICS
LABORATORY

Princeton Plasma Physics Laboratory
Report Disclaimers

Full Legal Disclaimer

Trademark Disclaimer

PPPL Report Availability

Princeton Plasma Physics Laboratory:

http://www.pppl.gov/techreports.cfm

Office of Scientific and Technical Information (OSTI):

http://www.osti.gov/scitech/

Related Links:

U.S. Department of Energy

Office of Scientific and Technical Information

Dependence of recycling and edge profiles on lithium evaporation in high triangularity, high performance NSTX H-mode discharges

R. Maingi[a], T.H. Osborne[b], M.G. Bell[a], R.E. Bell[a], D.P. Boyle[a], J.M. Canik[c], A. Diallo[a], R. Kaita[a], S.M. Kaye[a], H.W. Kugel[a], B.P. LeBlanc[a], S.A. Sabbagh[d], C.H. Skinner[a], V.A. Soukhanovskii[e], and the NSTX team

[a] *Princeton Plasma Physics Laboratory, Receiving 3, Route 1 North, Princeton, NJ 08543 USA*
[b] *General Atomics, 3550 General Atomics Ct., San Diego CA 92121, USA*
[c] *Oak Ridge National Laboratory, PO Box 2008, Oak Ridge TN 37831, USA*
[d] *Applied Physics and Applied Math Dept., Columbia University, New York, NY 10027 USA*
[e] *Lawrence Livermore National Laboratory, 7000 East Ave, P.O. Box 808, Livermore CA 94551, USA*

In this paper, the effects of a pre-discharge lithium evaporation scan on highly shaped discharges in the National Spherical Torus Experiment (NSTX) are documented. Lithium wall conditioning ('dose') was routinely applied onto graphite plasma facing components between discharges in NSTX, partly to reduce recycling. Reduced D_α emission from the lower and upper divertor and center stack was observed, as well as reduced midplane neutral pressure; the magnitude of reduction increased with the pre-discharge lithium dose. Improved energy confinement, both raw τ_E and H-factor normalized to scalings, with increasing lithium dose was also observed. At the highest doses, we also observed elimination of edge-localized modes. The midplane edge plasma profiles were dramatically altered, comparable to lithium dose scans at lower shaping, where the strike point was farther from the lithium deposition centroid. This indicates that the benefits of lithium conditioning should apply to the highly shaped plasmas planned in NSTX-U.

I. Introduction and Background

While many devices have reported performance improvements with lithium conditioning[1-6], including e.g. recent long pulse advances in EAST[7], the continuous improvement of plasma confinement and edge stability with *increasing* levels of lithium conditioning has been clearly documented in studies from the Natonal Spherical Torus Experiment (NSTX)[8-11]. Those first studies were conducted in discharges with a 'weaker' boundary shaping than typical in NSTX, namely an intermediate-level average triangularity ($\delta \sim 0.46$), low elongation ($\kappa \sim 1.8$), and relatively low squareness shape. Numerous studies have shown that strongly shaped discharges exhibit good performance in NSTX[12], and thus highly shaped discharges were chosen as the baseline configurations for NSTX-U[13, 14]. In this paper, we present trends from an experiment in NSTX in which pre-discharge lithium evaporation was systematically increased in highly shaped discharges ($\delta \sim 0.6$-0.7, $\kappa \sim 2.2$, high squareness), as envisioned for NSTX-U.

Lithium was introduced into NSTX prior to discharges with a pair of toroidally separated overhead lithium evaporator ("LiTER")[15]. Previous experiments have shown substantial reductions of the recycling light, improvements in global confinement[16-19], along with the appearance of ELM-free regimes[20], due to changes in the far edge density and pressure profiles[21]. The deuterium retention leading to the recycling reduction[22-24] has been correlated with possible segregation of oxygen impurities in the lithiated surface layers[25, 26]. The highly shaped discharges from the present study represented the first set into which lithium was introduced in this particular run period.

The centroid of the lithium deposition onto the lower divertor plasmas facing components (PFCs) from the LiTERs was on the inner-horizontal set of tiles, as shown in Figure 1; there was a Gaussian distribution of the deposition, with a full width of 23° in the poloidal cross section. Figures 1a and 1b illustrate the geometry of the inner and outer strike points with the centroid of LiTER deposition for the strongly shaped and weakly shaped discharges respectively. It is clear that the centroid is very near the outer strike point in strongly shaped discharges, and in the private flux region in weakly shaped ones. Thus it can be expected that this geometric difference could lead to a different effect on plasma discharges.

II. Trends as a function of pre-discharge lithium

A number of reference ELMy discharges over a range of neutral beam heating were taken prior to the introduction of lithium during this experiment. The range of pre-discharge evaporation ('dose') was from 120 mg to 570 mg; these equate to nominal peak coating thicknesses of ~60-300 nm, i.e. well in excess of the < 10 nm typical ion implantation depth for typical divertor T_e and T_i. Lithium dose in the first seven discharges averaged about 150 mg, and was increased to about 250 mg for the next eight discharges. Finally the dose was increased to about 450 mg for eleven discharges, and then increased to about 550 mg for the last nine discharges of the experiment. In a few instances the dose was lowered between otherwise comparable doses to inspect for signs of hysteresis. Additionally neutral beam power (P_{NBI}) was often modestly reduced with increasing dose, because the increase in confinement would otherwise have resulted in exceeding of the global beta limit, and subsequent minor or major disruption. Note that the reference

non-lithiated discharges used standard inter-discharge Helium Glow Discharge Cleaning for reproducibility, which was not needed when the lithium dose scan was initiated.

A comparison of discharges at two lithium doses (280 mg, 550 mg) and a reference ELMy discharge is shown in Figure 2. The steady P_{NBI} was 6 MW for the reference discharge, compared with 5 MW for the intermediate lithium dose, and 4 MW for the high lithium dose (panel 2b). Note that the reference and intermediate lithium discharges were well optimized. However, the highest lithium dose discharge was not fully optimized (due to available run time), which is reflected by the shorter realized pulse length. The time rate of increase of line average density dn/dt (panel (c)) from Thomson scattering data was indeed reduced with increasing lithium dose, while the normalized stored energy β_N (panel (d)) was comparable at ~ 6. Here $\beta_N=\beta_t B_t a_m/I_p$, where β_t is the average plasma pressure normalized to the on-axis vacuum toroidal field: $\beta_t=4\mu_0 W_{MHD}/(3V_p B_t^2)$. Also B_t is the toroidal field, a_m the minor radius, I_p the plasma current, W_{MHD} the stored energy from equilibrium reconstructions, V_p the plasma volume, and μ_0 the permittivity of free space. Both the raw energy confinement time τ_E and the value normalized to the ITERH97L global scaling law[27] increased with lithium dose (H97L shown in panel (e)). As also observed in the weakly shaped discharges, radiated power P_{rad} ramps during long ELM-free periods, which are triggered with the lithium, espcially at high doses (panels (f), (g)). Note also the substantial reduction in baseline D_α with lithium. In general, these observations are very similar to those at weaker shaping[8-11].

The trends of lower and upper divertor D_α, confinement relative to H97L scaling, and midplane neutral pressure with increasing lithium dose, are shown in Figure 3. The plots are color coded: the orange stars are from the present high shaping study, while the black diamonds are from the previous study in weakly shaped discharges[11]. The trends are, overall, rather comparable. A few points are noted. First, both datasets show a sharp decrease in lower divertor D_α, followed by a flattening at higher lithium dose (panel (a)).

We interpret this as the transition from the high recycling to sheath limited heat transport regimes. This transition occurs at lower lithium dose for the highly shaped discharges. This is qualitatively consistent with expectations, in that the strongly shaped discharges have the centroid of lithium deposition much closer to the outer strke point than the weakly shaped discharges. In other words, it takes less lithium dose to cause this transition. The final fractional reduction in lower divertor D_α is also larger in the highly shaped discharges (90% reduction, compared with ~ 70% in the weakly shaped discharges). There are other factors related to the X-point geometry, of course, but these differences seem qualitatively understandable. Second, the relative confinement improvement trend is similar, but the magnitude may be slightly lower in the highly shaped discharges (panel (c)). Additional data, including data at higher lithium dose, would be needed to determine if there were a real difference in the trends; for now, the plan is to conduct experiments over a wide range of lithium dose in NSTX-U. Finally the magnitude of the neutral pressure is markedly lower (by up to 50%) in the highly shaped discharges. The highly shaped discharges were closer to true double-null configuration, and thus may have had better isolation between the midplane and divertor than the lower

shaped discharges, which were biased more strongly toward the lower divertor.

III. Edge density and temperature profile changes

In addition to the global changes, the upstream plasma profiles change with increasing lithium dose in the highly shaped discharges. These changes are illustrated for three discharges with differing lithium dose in Figure 4, as a function of normalized poloidal flux ψ_N, where $\psi_N = (\psi_o - \psi(r))/(\psi_o - \psi_{sep})$ with ψ_o and- ψ_{sep} being the poloidal flux at the magnetic axis and separatrix respectively. The yellow arrows in the figure represent increasing lithium dose. Panel (a) shows that the n_e profile shifts inward with increasing lithium dose, while panel (b) shows that the T_i increases with increasing dose. Panel (c) shows that the near-separatrix T_e drops a little with increasing lithium dose, but that the T_e value for $\psi_N < 0.9$ increases substantially. The kinetic profiles were fit with 'standard' modified hyperbolic tangent functions[28], using a set of algorithms that allow selection of profiles as a function of the ELM cycle[29]. These fitted profiles for the total pressure are shown in panel (d): it can be seen that the far edge pressure decreases with increasing dose, whereas the pressure for $\psi_N < 0.85$ increases substantially. This is very similar to studies from the lower shaped discharges, which indicated improved edge stability with similar profile changes[10, 21]. In the previous studies, the individual density and temperature profiles changes appeared to be correlated to micro-tearing and electron temperature gradient mode stability[30]; it is likely that similar physics is present in the highly shaped discharges.

The advantage of higher shaping over lower shaping is access to higher I_p at the same B_t,

because of higher safety factor; this allows input of higher P_{NBI} before bumping up against global stability limits. The previous lower shaped discharges were limited to $I_p \leq$ 0.9 MA at 0.45 T; at the highest lithium dose ~ 700 mg, $P_{NBI} <$ 2.5-3 MW was required, as higher values resulted in $\beta_N >$ 5.5-6, i.e. above the global stability limit. For these strongly shaped discharges, $I_p \leq$ 1.2 MA at 0.45 T (in this experiment, $I_p =$ 1.0 MA), and $P_{NBI} \leq$ 4 MW was allowed, allowing access to β_N ~ 6. The difference in absolute edge parameters is shown in Figure 5, comparing a 2 MW discharge at low shaping with a 4 MW discharge at high shaping. Panel (a) shows very comparable n_e profiles; however the highly shaped discharge with higher P_{NBI} was able to access higher stable, T_e and T_i, and total pressure P_{e+i}. As NSTX-U is designed[13] to achieve a ~ 100% increase in I_p and B_t over NSTX, use of lithium conditioning bodes well for achieving good performance H-modes at the higher absolute plasma parameters.

IV. Summary and Conclusions

Discharge performance increased nearly continuously with increasing lithium dose in highly shaped discharges, as observed in previous NSTX studies in lower shaped discharges. The modest differences in the observed trends can be qualitatively understood by the more efficient deposition of lithium near the outer strike point in the highly shaped discharges. These results bode well for the use of lithium conditioning onto graphite PFCs in NSTX-U, which will be equipped with four lithium evaporators, to coat *both* the lower and upper divertors, extending the lower divertor coating capability in NSTX.

Acknowledgements

Center of LITER deposition

(a)

Outer Strike Point

(b)
Center of LITER deposition
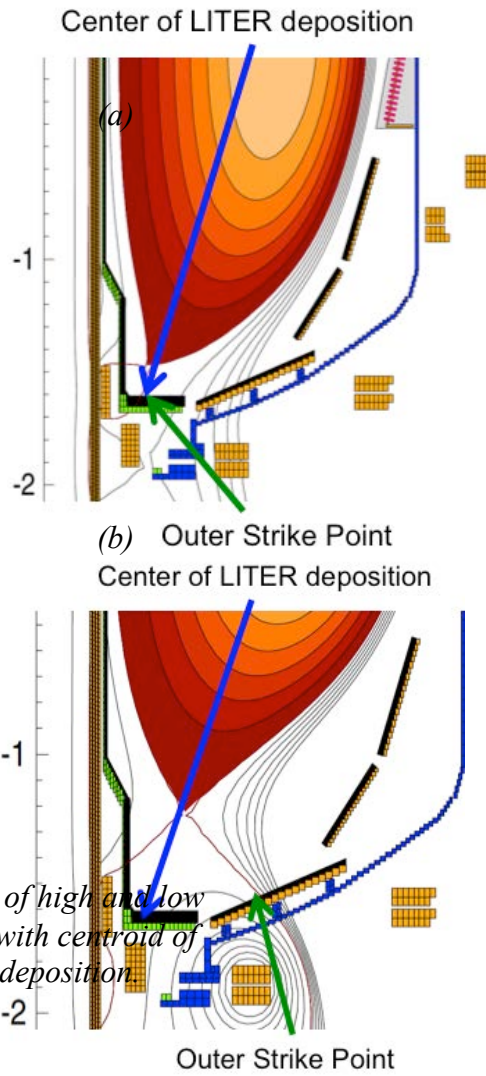
Fig. 1: comparison of high and low
shapes (a and b) with centroid of
lithium evaporator deposition

Outer Strike Point

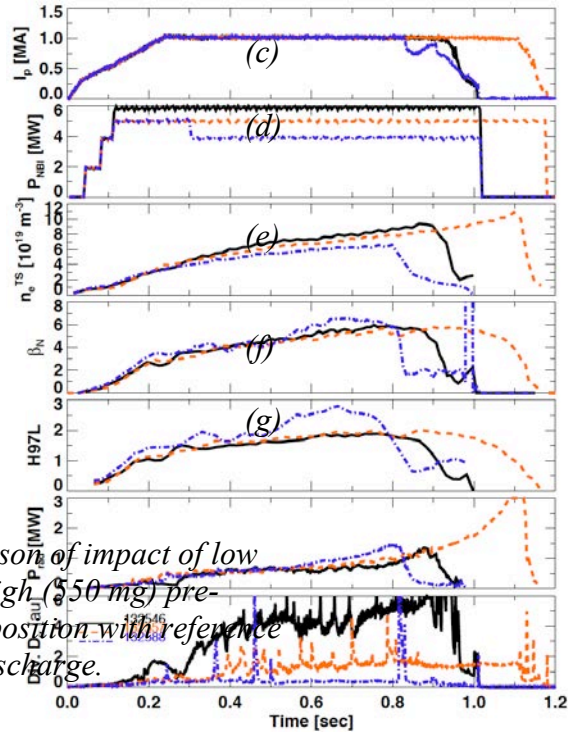0 mg *280 mg* *550 mg*   *(a)*

(b)

(c)

(d)

(e)

(f)

(g)

Fig. 2: comparison of impact of low (280 mg) and high (550 mg) pre-discharge li deposition with reference non-lithiated discharge.

(a)   *(c)*
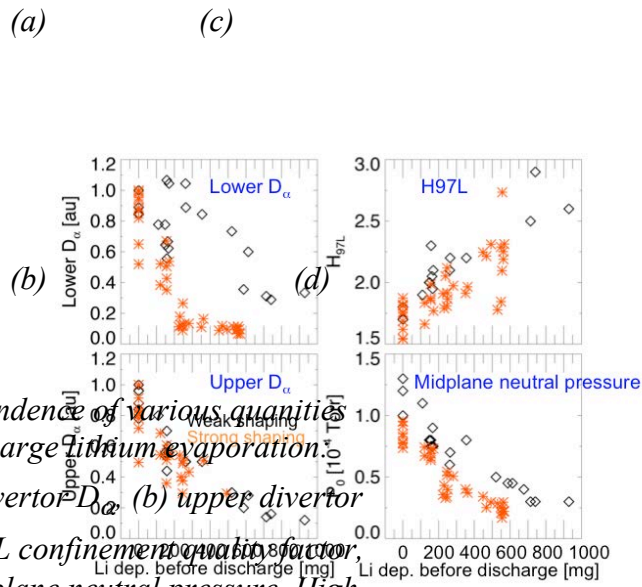
(b)   *(d)*

Fig. 3: dependence of various quanities
on pre-discharge lithium evaporation:
(a) lower divertor D_α, (b) upper divertor
D_α, (c) H97L confinement quality factor,
and (d) midplane neutral pressure. High
and low δ discharges are color coded.
Panels (a), (b), and (c) are taken near
?00msec, while panel (c) is evaluated at
the peak of the stored energy during the
discharge.

(a)

(c)

(b)

(d)

0 mg – 6 MW
150 mg – 5 MW
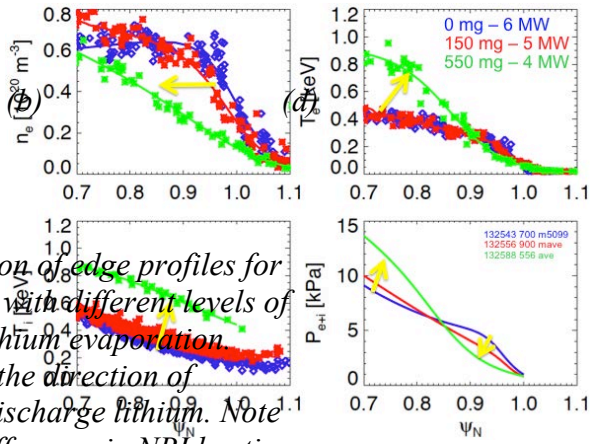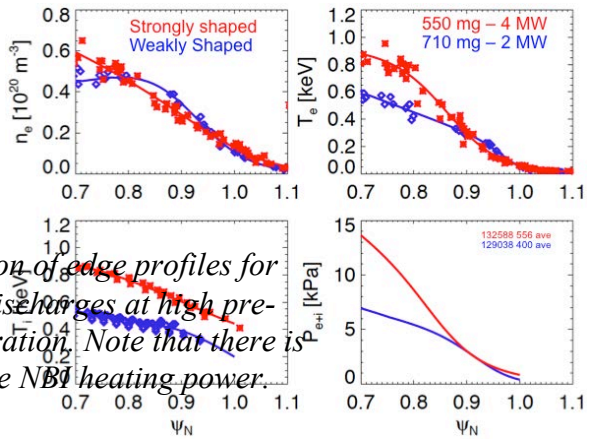550 mg – 4 MW

132543 700 m5099
132556 900 mave
132588 556 ave

Fig. 4: comparison of edge profiles for three discharges with different levels of pre-discharge lithium evaporation. Arrows indicate the direction of increasing pre-discharge lithium. Note that there is a difference in NBI heating power also.

Fig. 5: comparison of edge profiles for high and low δ discharges at high pre-discharge evaporation. Note that there is difference in the NBI heating power.

References

[1] Snipes J., E.S. Marmar, and Terry J. L., 1992 *J. Nucl. Mater.* 196-198 686

[2] Mansfield D. K., *et al.*, 2001 *Nucl. Fusion* 41 1823

[3] Majeski R., *et al.*, 2006 *Phys. Rev. Lett.* 97 075002

[4] Apicella M., *et al.*, 2007 *J. Nucl. Mater.* 363-365 1346

[5] Sánchez J., *et al.*, 2009 *J. Nucl. Mater.* 390-391 852

[6] ZUO G.Z., *et al.*, 2010 *Fusion Science and Technology* 12 646

[7] Guo H. Y., *et al.*, 2014 *Nucl. Fusion* 54 013002

[8] Maingi R., *et al.*, 2011 *Phys. Rev. Lett.* 107 145004

[9] Canik J. M., *et al.*, 2011 *Phys. Plasmas* 18 056118

[10] Boyle D. P., *et al.*, 2011 *Plasma Phys. Control. Fusion* 53 105011

[11] Maingi R., *et al.*, 2012 *Nucl. Fusion* 52 083001

[12] Gates D. A., *et al.*, 2006 *Phys. Plasmas* 13 056122

[13] Menard J. E., *et al.*, 2012 *Nucl. Fusion* 52 083015

[14] Gerhardt S. P., Andre R., and Menard J. E., 2012 *Nucl. Fusion* 52 083020

[15] Kugel H. W., *et al.*, 2009 *J. Nucl. Mater.* 390-391 1000

[16] Kugel H. W., *et al.*, 2008 *Phys. Plasmas* 15 056118

[17] Bell M. G., *et al.*, 2009 *Plasma Phys. Control. Fusion* 51 124054

[18] Ding S., *et al.*, 2010 *Plasma Phys. Control. Fusion* 52 015001

[19] Kaye S. M., *et al.*, 2013 *Nucl. Fusion* 53 063005

[20] Mansfield D. K., *et al.*, 2009 *J. Nucl. Mater.* 390-391 764

[21] Maingi R., *et al.*, 2009 *Phys. Rev. Lett.* 103 075001

[22] Smirnov R. D., *et al.*, 2010 *Contributions to Plasma Physics* 50 299

[23] Canik J. M., *et al.*, 2011 *J. Nucl. Mater.* 415 S409

[24] Boyle D., *et al.*, 2013 *J. Nucl. Mater.* 438 S979

[25] Taylor C. N., *et al.*, 2013 *Fusion Eng. Des.* 88 3157

[26] Krstic P. S., *et al.*, 2013 *Phys. Rev. Lett.* 110 105001

[27] Kaye S. M. and group t. I. c. d. w., 1997 *Nucl. Fusion* 37 1303

[28] Groebner R. J. and Osborne T. H., 1998 *Phys. Plasmas* 5 1800

[29] Osborne T. H., *et al.*, 2008 *J. Phys.: Conf. Series* 123 012014

[30] Canik J. M., *et al.*, 2013 *Nucl. Fusion* 53 113016

Princeton Plasma Physics Laboratory
Office of Reports and Publications

Managed by
Princeton University

under contract with the
U.S. Department of Energy
(DE-AC02-09CH11466)